Coherently stimulated parametric down-conversion, phase effects, and quantum-optical interferometry

Richard Birrittella, Anna Gura, and Christopher C. Gerry
Department of Physics and Astronomy, Lehman College, The City University of New York, Bronx, New York 10468-1589, USA
(Received 13 November 2014; revised manuscript received 16 March 2015; published 5 May 2015)

We re-examine the properties of the states produced by nondegenerate coherently stimulated parametric down-conversion wherein the signal and idler modes are seeded with coherent states of light and where the nonlinear crystal is driven by a strong classical field as described by the parametric approximation. The states produced are the two-mode squeezed coherent states defined with a specific ordering of operators, namely, the displacement operators of the two modes acting on the double vacuum state followed by the action of the two-mode squeeze operator representing the down-conversion process. Though mathematically equivalent to the reverse ordering of operators, but with different displacement parameters, the ordering we consider is closely related to what could most easily be implemented in the laboratory. The statistical properties of the state are studied with an emphasis on how they, and its average photon number, are affected by the various controllable phases, namely, those of the classical pump field of the two input coherent states. We then consider the multiphoton interference effects that arise if the two beams are overlapped on a 50:50 beam splitter, investigating the role of the phases in controlling the statistical properties of the output states. Finally, we study the prospects for the application of the states to quantum-optical interferometry to obtain sensitivities in phase-shift measurements beyond the standard quantum limit.

DOI: 10.1103/PhysRevA.91.053801 PACS number(s): 42.50.St, 42.25.Hz

I. INTRODUCTION

For many years now, parametric down-conversion has been a laboratory source of light with strong nonclassical properties [1]. The generated states of light have been used to study a variety of quantum effects and have had applications for fundamental tests of quantum mechanics as in two-photon interference at a beam splitter [2] and to Bell-type inequalities [3], as well as practical applications such as to quantum metrology [4], quantum information processing [5], and quantum imaging [6]. In almost all cases studied so far in the laboratory, the light produced is the result of spontaneous down-conversion. That is, a strong classical (UV) pump field drives a nonlinear crystal producing pairs of frequency down-converted (infrared) photons into the signal and idler modes initially in vacuum states. The state produced is the two-mode squeezed vacuum state (TMSVS) [7], which consists of a superposition of products of identical (twin) Fock states of the signal and idler modes, where the photon-number distributions for the reduced density operators for each of the modes is thermal [8]. For low gain, spontaneous down-conversion produces mostly vacuum states in the output signal and idler modes with about 1 in 10^{12} pump photons converting to a signal-idler pair of photons. This process was employed in the famous Hong-Ou-Mandel experiment [2], for example.

On the other hand, if the signal and idler modes into the down-converter are initially fed beams of coherent light, the light produced is the two-mode squeezed coherent state (TMSCS) and the process producing it is called coherently stimulated down-conversion, or sometimes *seeded* parametric down-conversion. The statistical properties of these states were discussed in the literature some years ago by Caves *et al.* [9] and by Selvadoray *et al.* [10]. It is the latter authors who have performed the most complete analysis of the states by considering complex displacement and squeezing parameters. Recently, this light source has been suggested for applications to quantum interferometric photolithography [11] and to quantum-optical interferometry [4].

In this paper we first re-examine the TMSCS. The effects of the choices of the phases of the two input coherent states and of the classical pump field, individually and in combination, are studied as a means of controlling the properties of the output fields. Our motivation comes from the possible applications of such states to photon-number parity–based quantum-optical interferometry. Previously, Kolkiran and Agarwal [12] studied quantum-optical interferometry using high-gain coherently stimulated down-conversion. In that work, however, they did not study the statistical properties of the states before and after beam splitting, nor did they study the use of photon-number parity measurements for interferometry or the related issue of the Cramer-Rao bound based on the quantum Fisher information for optimal sensitivity. These issues are addressed in the present paper.

In the literature [9,10], the TMSCS are mathematically defined in two ways having to do with the orderings of the two-mode squeeze and the displacement operators acting on the double vacuum state. The states generated are mathematically equivalent but differ in their implied methods of physical generation. From an experimental point of view, we believe that the natural way to think about the states is to assume coherent light beams are fed into the input signal and idler modes of the down-converter, which then acts to squeeze those input states—hence the states are the result of coherently stimulated down-conversion. As the coherent states may be defined as displaced vacuum states, it follows that the TMSCS is mathematically defined by the action of the displacement operators on the vacuum states of each mode followed by the action of the two-mode squeeze operator. However, in the literature, specifically the papers of Caves *et al.* [9] and Selvadoray *et al.* [10] cited above, one finds a definition of the TMSCS with the operators acting in reverse

order, i.e., with the two-mode squeeze operator acting on the double vacuum followed by the displacement operator such that the states generated could be called two-mode displaced squeezed vacuum states (TMDSVS). Of course, the definitions are mathematically equivalent with properly chosen displacement parameters, but physically the latter states are generated by performing independent displacements on the two modes of the two-mode squeezed vacuum. That does not appear to be an attractive method for generating the states in the laboratory in view of the fact that displaced vacuum states (coherent states) are readily available from well phase-stabilized lasers. But as we shall discuss below, the two definitions can lead to misconceptions, or at least confusion, about the roles that the various phases (pump and coherent state) play in controlling the statistical properties of the states and on how the beams transform upon being mixed at a beam splitter. Specifically, in the case of the TMDSVS, the phases are in some sense hidden. For the purposes of interferometry, it is desirable that the beam splitter create a balanced, well separated, bimodal joint photon-number distribution, and we show that such is possible by judicious choices of the relevant phases and a certain combination of the phases.

The paper is organized as follows: In Sec. II we briefly review the two-mode squeezed states and their production by spontaneous down-conversion. In Sec. III we discuss coherently stimulated down-conversion and the statistical properties of the TMSCS produced. In Sec. IV we discuss the multiphoton interference and the consequent transformation of our state by a 50:50 beam splitter and the control of the outcome of the process by the choices of the various phases. In Sec. V we examine, for certain choices of parameters, the efficacy of the states for performing substandard-quantum-limited quantum-optical interferometry through the use a photon-number parity measurements. It is known that minimum phase uncertainty for a given input state is given by the corresponding Cramer-Rao bound [13], which in turn is determined by the quantum Fisher information [14], and that, in all cases studied so far, photon-number parity measurements saturate this bound. In Sec. VI we finish the paper with a summary and some brief remarks. Some mathematical results are included in an Appendix.

II. COHERENTLY STIMULATED PARAMETRIC DOWN-CONVERSION AND THE TWO-MODE SQUEEZED COHERENT STATES

We begin by writing down the two-mode squeeze operator

$$\hat{S}(z) = \exp(z^*\hat{a}\hat{b} - z\hat{a}^\dagger\hat{b}^\dagger), \quad z = re^{2i\phi}, \tag{1}$$

where r is the so-called squeezing parameter, $0 \leqslant r < \infty$, and where 2ϕ is the phase of the pump field, treated classically here, driving the down-conversion process. (We have parameterized this phase as 2ϕ to be consistent with the convention used in the literature.) Here $(\hat{a},\hat{a}^\dagger)$ and $(\hat{b},\hat{b}^\dagger)$ are the Bose operators representing the signal and idler modes, respectively. For an arbitrary two-mode input state $|\psi_{\rm in}\rangle$, the output state will be given by $|\psi_{\rm out}\rangle = \hat{S}(z)|\psi_{\rm in}\rangle$. The average total photon number of the output state will be given by

$$\begin{aligned}\bar{n}_{\rm total} &= \langle\psi_{\rm in}|\hat{S}^\dagger(z)(\hat{a}^\dagger\hat{a} + \hat{b}^\dagger\hat{b})\hat{S}(z)|\psi_{\rm in}\rangle \\ &= \langle\psi_{\rm in}|[(\hat{a}^\dagger\hat{a} + \hat{b}^\dagger\hat{b})\cosh(2r) - (e^{2i\phi}\hat{a}^\dagger\hat{b}^\dagger + e^{-2i\phi}\hat{a}\hat{b}) \\ &\quad \times \sinh(2r) + 2\sinh^2 r]|\psi_{\rm in}\rangle, \end{aligned} \tag{2}$$

where we have used the operator relations

$$\hat{S}^\dagger(z)\begin{pmatrix}\hat{a}\\ \hat{b}\end{pmatrix}\hat{S}(z) = \begin{pmatrix}\hat{a}\cosh r - e^{2i\phi}\hat{b}^\dagger\sinh r\\ \hat{b}\cosh r - e^{2i\phi}\hat{a}^\dagger\sinh r\end{pmatrix}. \tag{3}$$

Of course, if the input put state is just the pair vacuum state $|\psi_{\rm in}\rangle = |0\rangle_a|0\rangle_b$ the output will be the TMSVS,

$$\begin{aligned}|\psi_{\rm out}\rangle = |\xi\rangle &= (1-|\xi|^2)^{1/2}\sum_{n=0}^{\infty}\xi^n|n\rangle_a|n\rangle_b \\ &= \frac{1}{\cosh r}\sum_{n=0}^{\infty}(-1)^n e^{2in\phi}\tanh^n r|n\rangle_a|n\rangle_b, \end{aligned} \tag{4}$$

where $\xi = -e^{2i\phi}\tanh r$, for which the average total photon number is given by

$$\bar{n}_{\rm total} = 2\sinh^2 r, \tag{5}$$

which, it should be noted, is independent of the pump phase 2ϕ. The photon states of each mode are tightly correlated and the state as a whole is highly nonclassical due the presence of squeezing in one or the other of the superposition quadrature operators of the combined modes. On the other hand, the photon-number statistics are super-Poissonian in each mode. The joint photon-number probability distribution for there being n_1 photons in mode a and n_2 in mode b is

$$P(n_1,n_2) = |\langle n_1|\langle n_2|\xi\rangle|^2 = \frac{\tanh^{2n} r}{\cosh^2 r}\delta_{n_1,n}\delta_{n_2,n}, \tag{6}$$

such that only the "diagonal" elements $n_1 = n_2 = n$ are nonzero. In fact, each mode separately has thermal-like statistics.

The two-mode squeezing operation is realized by the interaction picture evolution operator given in the interaction picture as

$$\hat{U}_{\rm I}(t) = \exp[-i\hat{H}_{\rm I}t/\hbar], \tag{7}$$

where the interaction Hamiltonian under the parametric approximation is given by [15]

$$\hat{H}_{\rm I} = i\hbar(\gamma\hat{a}\hat{b} - \gamma^*\hat{a}^\dagger\hat{b}^\dagger). \tag{8}$$

The parameter γ is proportional to the second-order nonlinear susceptibility $\chi^{(2)}$ and to the amplitude and phase factor of the driving laser field, here assumed to be a strong classical field such that depletion and fluctuations in the field can be ignored as per the parametric approximation. Writing $\gamma = |\gamma|e^{2i\phi}$ the squeeze operator becomes [7]

$$\hat{S}(z) = \exp[-i\hat{H}_{\rm I}t/\hbar] = \exp[r(\hat{a}\hat{b}e^{-2i\phi} - \hat{a}^\dagger\hat{b}^\dagger e^{2i\phi})], \tag{9}$$

where the squeeze parameter $r = |\gamma|t$, which one can take as a scaled dimensionless time.

We now turn to a discussion of the TMSCS, which we take to be the output state for an input state consisting of

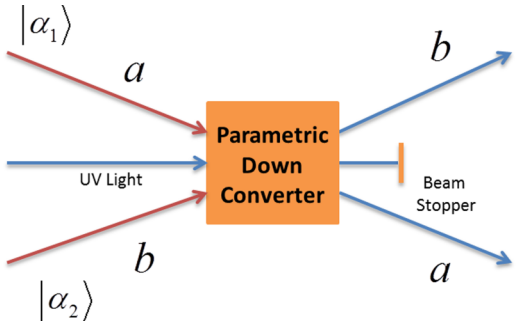

FIG. 1. (Color online) A sketch of the scheme for generating two-mode squeezed coherent states where signal and idler modes (a and b, respectively) prepared in coherent states are fed into the parametric down-converter.

a product of coherent states, i.e., $|\psi_{\rm in}\rangle = |\alpha_1\rangle_a|\alpha_2\rangle_b$ so that $|\psi_{\rm out}\rangle \equiv |\xi;\alpha_1,\alpha_2\rangle$, where

$$|z;\alpha_1,\alpha_2\rangle = \hat{S}(z)\,|\alpha_1\rangle_a|\alpha_2\rangle_b = \hat{S}(z)\,\hat{D}(\alpha_1,\alpha_2)\,|0\rangle_a|0\rangle_b \tag{10}$$

and where $\hat{D}(\alpha_1,\alpha_2) = \hat{D}_a(\alpha_1)\hat{D}_b(\alpha_2)$ is the product of the displacement operators of each of the modes:

$$\begin{aligned}\hat{D}_a(\alpha_1) &= \exp(\alpha_1\hat{a}^\dagger - \alpha_1^*\hat{a}),\\ \hat{D}_b(\alpha_2) &= \exp(\alpha_2\hat{b}^\dagger - \alpha_2^*\hat{b}).\end{aligned} \tag{11}$$

The coherent states are generated from the vacuum by the actions of the displacement operators such that $|\alpha_1\rangle_a|\alpha_2\rangle_b = \hat{D}(\alpha_1,\alpha_2)|0\rangle_a|0\rangle_b$ where

$$|\alpha\rangle = \hat{D}(\alpha)\,|0\rangle = e^{-|\alpha|^2/2}\sum_{n=0}^{\infty}\frac{\alpha^n}{\sqrt{n!}}\,|n\rangle\,. \tag{12}$$

The TMSCS given by Eq. (10) are generated by feeding the coherent states $|\alpha_1\rangle_a|\alpha_2\rangle_b$ to the input signal and idler modes, respectively, of the down-converter as illustrated in Fig. 1 and hence the process is coherently stimulated down-conversion. The average total photon number for the state of Eq. (10) is given by

$$\begin{aligned}\bar{n}_{\rm total} &= {}_a\langle\alpha_1|_b\langle\alpha_2|[(\hat{a}^\dagger\hat{a}+\hat{b}^\dagger\hat{b})\cosh(2r)\\ &\quad -(\hat{a}\hat{b}e^{-2i\phi}+\hat{a}^\dagger\hat{b}^\dagger e^{2i\phi})\sinh(2r)+2\sinh^2 r]|\alpha_1\rangle_a|\alpha_2\rangle_b\\ &= (|\alpha_1|^2+|\alpha_2|^2)\cosh(2r)\\ &\quad -(e^{2i\phi}\alpha_1^*\alpha_2^*+e^{-2i\phi}\alpha_1\alpha_2)\sinh(2r)+2\sinh^2 r,\end{aligned} \tag{13}$$

where we have used the results of Eq. (2) and that

$$\hat{D}^\dagger(\lambda)\hat{a}\hat{D}(\lambda) = \hat{a}+\lambda, \quad \hat{D}^\dagger(\lambda)\hat{a}^\dagger\hat{D}(\lambda) = \hat{a}^\dagger+\lambda^*. \tag{14}$$

If we now set $\alpha_1 = |\alpha_1|e^{i\theta_1}$ and $\alpha_2 = |\alpha_2|e^{i\theta_2}$, we have

$$\begin{aligned}\bar{n} &= (|\alpha_1|^2+|\alpha_2|^2)\cosh(2r)\\ &\quad -2|\alpha_1||\alpha_2|\cos(\Phi)\sinh(2r)+2\sinh^2 r,\end{aligned} \tag{15}$$

where $\Phi = \theta_1+\theta_2-2\phi$. Evidently, the average photon number for the TMSCS depends on the combination of the phases θ_1,θ_2, and 2ϕ in Φ. This result is not new [1], but as far as we are aware, the effect of the phases on the average photon number in coherently stimulated parametric down-conversion, as given in Eq. (15), has yet to be demonstrated experimentally. The joint photon-number distribution also depends only on the value of Φ. However, as we demonstrate below, the joint photon-number distribution obtained *after* the two beams are mixed at a 50:50 beam splitter depends on the individual values of the phases, not just on the combination Φ.

In the literature, one often finds the TMSCS defined according to the reverse ordering of the squeeze and displacement operators operating on the vacuum that was used above. That is, one encounters the definition

$$|\beta_1,\beta_2;z\rangle \equiv \hat{D}(\beta_1,\beta_2)\hat{S}(z)|0\rangle_a|0\rangle_b, \tag{16}$$

where $\beta_1 = |\beta_1|e^{i\psi_1}$ and $\beta_2 = |\beta_2|e^{i\psi_2}$ are, for the moment, arbitrary "coherent" amplitudes with phases ψ_1 and ψ_2. The average total photon number obtained for this representation is given by

$$\begin{aligned}\bar{n}_{\rm total} &= \langle\beta_1,\beta_2;z|(\hat{a}^\dagger\hat{a}+\hat{b}^\dagger\hat{b})|\beta_1,\beta_2;z\rangle\\ &= {}_a\langle 0|_b\langle 0|\hat{S}^\dagger(z)\hat{D}^\dagger(\beta_1,\beta_2)(\hat{a}^\dagger\hat{a}+\hat{b}^\dagger\hat{b})\\ &\quad\times\hat{D}(\beta_1,\beta_2)\hat{S}^\dagger(z)|0\rangle_a|0\rangle_b\\ &= |\beta_1|^2+|\beta_2|^2+2\sinh^2 r,\end{aligned} \tag{17}$$

where we have used the results of Eqs. (14) and (3) in that order. The total photon number in this case displays no dependence on the phases ψ_1, ψ_2, and 2ϕ. However, the two representations of the TMSCS are equivalent provided

$$\hat{S}(z)\hat{D}(\alpha_1,\alpha_2)\hat{S}^\dagger(z) = \hat{D}(\beta_1,\beta_2), \tag{18}$$

which holds if

$$\beta_1 = \mu\alpha_1-\nu\alpha_2^*, \quad \beta_2 = \mu\alpha_2-\nu\alpha_1^*, \tag{19}$$

where $\mu = \cosh r$ and $\nu = e^{2i\phi}\sinh r$. The inverse transformations, needed for later, are

$$\alpha_1 = \mu\beta_1+\nu\beta_2^*, \quad \alpha_2 = \mu\beta_2+\nu\beta_1^*. \tag{20}$$

Thus under these conditions $|z;\alpha_1,\alpha_2\rangle$ and $|\beta_1,\beta_2;z\rangle$ are identical states but represent different methods of generation. As mentioned, the former states result from the action of the down-converter on input coherent states while the latter are displaced TMSVS, i.e., they require displacement operations on both modes of a TMSVS.

As just discussed, our result for the average photon number calculated for representation of the state as given by $|\beta_1,\beta_2;z\rangle$ is independent of the phases ψ_1, ψ_2, and 2ϕ. That is, there is no *explicit* phase dependence here. However, because of the transformations of Eqs. (19) and (20), there is an *implicit* dependence on the phases θ_1,θ_2, and 2ϕ which show up in the combination $\Phi = \theta_1+\theta_2-2\phi$ in Eq. (15). In this sense, the phase dependence of Eq. (15) is "hidden." Caves *et al.* [9] and Selvadoray *et al.* [10] use the definition of Eq. (16) for the TMSCS, though the latter authors, for calculational convenience, also use the definition given by Eq. (10). Our result in Eq. (17) agrees with that of Selvadoray *et al.* [10], who point out that $\bar{n}$ is insensitive to a certain combination of angles, that here we shall call Ψ, which, in our notation, has the form $\Psi = \psi_1+\psi_2-2\phi$. In the Appendix we show the relationship between the angles Φ and Ψ, and we also show the relationships between the sets of angles (θ_1,θ_2) and (ψ_1,ψ_2). The result in Eq. (15) is not inconsistent with the result of Eq. (17) as long as the relations of Eqs. (19) and (20) hold.

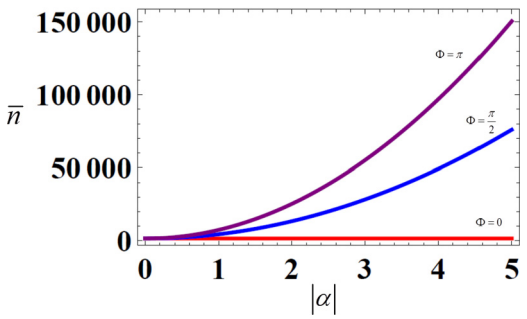

FIG. 2. (Color online) $\bar{n}$ versus $|\alpha|$ for $r=4$, for $\Phi=0,\pi/2$, and π.

The essential point here is that the phases of the pump field and of the input coherent states, through Φ, can be adjusted so as to exert control over the average photon number of the output field of the down-converter and of the statistics of this field, as will be discussed below. The dependence on the phases is hidden in the expression for the average photon number as given in Eq. (15), though it is carried along through Eq. (19). For given values of $|\alpha_1|,|\alpha_2|$ and r, the average photon number can vary significantly by adjusting Φ, as we show in Fig. 2 for the choices $|\alpha_1|=|\alpha_2|=|\alpha|$ and for $r=4$. Note that for $\Phi=0$ the average photon number is essentially independent of the coherent state amplitude $|\alpha|$. It is easy to see why. For the choices $|\alpha_1|=|\alpha_2|=|\alpha|$ we can rewrite Eq. (15) as

$$\bar{n}=2|\alpha|^2[\cosh(2r)-\cos(\Phi)\sinh(2r)]+2\sinh^2 r, \tag{21}$$

and for $\Phi=0$ the bracket term $\cosh(2r)-\sinh(2r)\to 0$ for sufficiently high r. We are then left with the dominant contribution, $\bar{n}=2\sinh^2 r$, which is identical with the average photon number for the squeezed vacuum state. Obviously we can maximize $\bar{n}$ for the choice $\Phi=\pi$. As we show below, these different choices of Φ dramatically affect the nature of the photon-number distributions both before and after beam splitting. We also point out that for a fixed value of Φ, different arrangements and values of the corresponding angles θ_1,θ_2, and 2ϕ affect the joint photon-number distribution after beam splitting, but not before. We note that Caves *et al.* [9], who examined the TMSCS as defined through Eq. (16), set $\phi=0$, stating that this can be done "without loss of generality." This is misleading as should be clear from the above discussion.

We now proceed to write down the quantum amplitudes and photon distributions associated with the states $|z;\alpha_1,\alpha_2\rangle$. In terms of the numbers states,

$$|z;\alpha_1,\alpha_2\rangle=\sum_{n_1=0}^{\infty}\sum_{n_2=0}^{\infty}c(n_1,n_2)|n_1\rangle_a|n_2\rangle_b. \tag{22}$$

At this point it is useful to convert our two-mode number state labeling to the angular momentum states $|j,m\rangle$ such that we have the mapping [16]

$$|n_1\rangle_a|n_2\rangle_b=|j,m\rangle,\ \text{for}\ j=\frac{(n_1+n_2)}{2}\quad\text{and}\quad m=\frac{(n_1-n_2)}{2}. \tag{23}$$

We can rewrite our two-mode squeezed coherent states in terms of the angular momentum states as

$$|z;\alpha_1,\alpha_2\rangle=\sum_{j=0,\frac{1}{2},1,\ldots}^{\infty}\sum_{m=-j}^{m}c(j+m,j-m)|j,m\rangle, \tag{24}$$

where, adapting (and correcting) a result obtained by Selvadoray *et al.* [10], the coefficients are given by

$$\begin{aligned}c(j+m,j-m)&=\exp[-i\pi(j-|m|)]\left[\frac{(j-|m|)!}{(j+|m|)!}\right]^{1/2}\left[\frac{\alpha_1\alpha_2}{\mu\nu}\right]^{|m|}\frac{1}{\mu}\left(\frac{\nu}{\mu}\right)^j\\&\times L_{j-|m|}^{2|m|}\left(\frac{\alpha_1\alpha_2}{\mu\nu}\right)\left(\frac{\alpha_1}{\alpha_2}\right)^m\\&\times\exp\left[-\frac{1}{2}(|\alpha_1|^2+|\alpha_2|^2)\right]\exp\left(\frac{\nu^*\alpha_1\alpha_2}{\mu}\right),\end{aligned} \tag{25}$$

and where it is to be understood that $n_1=j+m$ and $n_2=j-m$, and where, again, $\mu=\cosh r$ and $\nu=e^{2i\phi}\sinh r$. The functions $L_n^k(x)$ are associated Laguerre polynomials. In terms of the phases θ_1,θ_2, and ϕ, the amplitude of Eq. (25) can written as

$$\begin{aligned}&c(j+m,j-m)\\&\quad=\exp[-i\pi(j-|m|)]\left[\frac{(j-|m|)!}{(j+|m|)!}\right]^{1/2}\\&\qquad\times\left[\frac{2|\alpha_1||\alpha_2|}{\sinh(2r)}\right]^{|m|}\frac{\tanh^j r}{\cosh r}\exp[i(|m|\Phi+2j\phi)]\\&\qquad\times L_{j-|m|}^{2|m|}\left(\left[\frac{2|\alpha_1||\alpha_2|}{\sinh(2r)}\right]\exp(i\Phi)\right)\left(\frac{|\alpha_1|}{|\alpha_2|}\right)^m\\&\qquad\times\exp[im(\theta_1-\theta_2)]\exp\left[-\frac{1}{2}(|\alpha_1|^2+|\alpha_2|^2)\right]\\&\qquad\times\exp[\exp(i\Phi)|\alpha_1||\alpha_2|\tanh r].\end{aligned} \tag{26}$$

There are two things to note regarding the dependence of these amplitudes on the various phases. The first is the appearance of the combination $\Phi=\theta_1+\theta_2-2\phi$. As noted above, the average total photon number for the two beams in this representation depends only on Φ. This is a reflection of the fact that the joint photon-number statistics depend only on Φ, as the probability for finding n_1 photons in mode a and n_2 in mode b is given by

$$P(n_1,n_2)=|c(n_1,n_2)|^2, \tag{27}$$

as is clear from an examination of the coefficients given by Eq. (26).

We now consider the joint photon-number probability distributions for the TMSCS for various values of state parameters. In Fig. 3 we plot $P(n_1,n_2)$ versus n_1 and n_2 for the fixed values $r=1.2$ and $\alpha_1=\alpha_2$ but for the choices $\Phi=0,\pi/2$, and π. The distribution is populated about the line $n_1=n_2$ (as is true for the TMSVS), and the effect of the phase Φ on the distribution is clear as the peak of the distribution migrates along the aforementioned line in accordance with the change in the total average photon number as the phase angle changed.

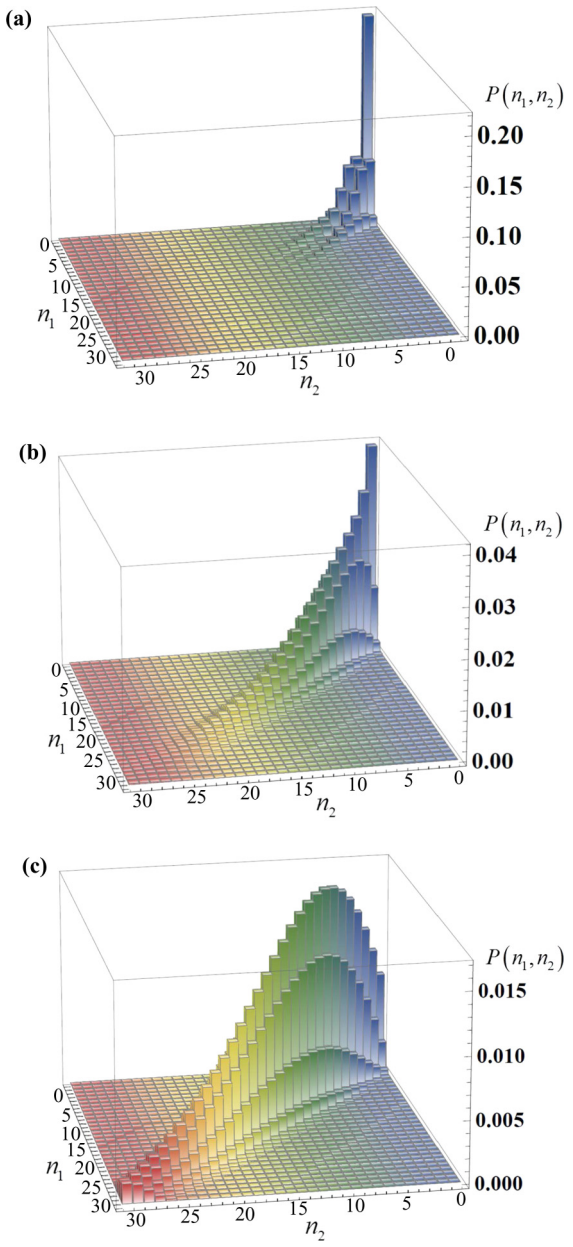

FIG. 3. (Color online) Joint photon-number distribution $P(n_1, n_2)$ versus n_1 and n_2 for the two-mode squeezed coherent states for $r = 1.2$ and $\alpha_1 = \alpha_2 = 1$ for (a) $\Phi = 0$, (b) $\Phi = \pi/2$, and (c) $\Phi = \pi$.

We have seen that for fixed values of the squeezing parameter and coherent state amplitudes the average photon number and the shapes of the joint photon-number distribution change with the phase Φ. Of course, this suggests that other quantities change with the phase as well. We consider here only the effect of the phase on the degree of entanglement between the two modes. We use the linear entropy

$$S = 1 - \mathrm{Tr}_{a(b)}\hat{\rho}^2_{a(b)}, \tag{28}$$

where $\hat{\rho}_{a(b)} = \mathrm{Tr}_{b(a)}\hat{\rho}$ is the reduced density operator for the $a(b)$ mode. Entanglement becomes maximum for $S = 1$. In Fig. 4 we show the linear entropy as a function of the phase Φ for the fixed values $r = 1.7$ and $|\alpha_1| = |\alpha_2| = 2$. We see

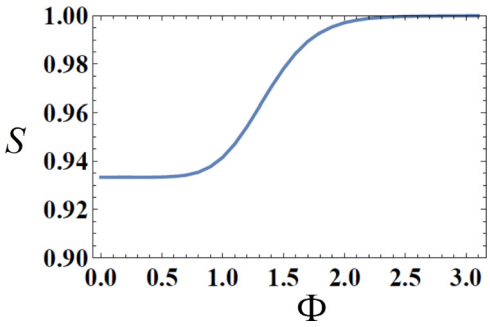

FIG. 4. (Color online) Plot of the linear entropy S against the phase Φ for $r = 1.7$ and $|\alpha_1| = |\alpha_2| = 2$.

that the entanglement is high for all values of the phase Φ, but it is at the maximum $S = 1$ for $\Phi = \pi$, the same phase that maximizes the average photon number for a given squeeze parameter and coherent state amplitudes.

As pointed out above, only the choice of the phase angle Φ affects the distribution; the choices of θ_1,θ_2, and ϕ individually do not affect the distribution. They also do not affect the linear entropy. However, as we show in the next section, the individual phases can affect the outcome of mixing the two beams at a beam splitter.

To conclude this section we wish to draw the reader's attention to Fig. 2 of the paper by Selvadoray *et al.* [10]. There they plot photon-number distributions for (in our notation) $\beta_1 = \beta_2 = 7$,$r = 4$, for various values of the phase combination we call Ψ. The average photon number of their state is $\bar{n} = 1\,587.4$, yet they display their distributions only out as far as $n_1 = n_2 = 100$, thus apparently not including most of the distribution, especially that part of it near the average $n_1 \approx \bar{n}/2 \approx n_2$. However, the full distribution in such cases is very broad and also very flat so that the oscillations close to the origin observed are their most interesting features. It turns out that for $\Psi = 0$ the corresponding values of α_1 and α_2 are both $\sim$380. On the other hand, for $\Psi = \pi$ the corresponding values of α_1 and α_2 are $\sim$0.127, indicating that from the point of view given by the state definition Eq. (10), the corresponding state is very close to the two-mode squeezed vacuum, and this explains why it is concentrated along the diagonal precisely as shown in Fig. 2(a) of Selvadoray *et al.* [10] for this choice of the phase Ψ. The point here is that the relevant state parameters (α_1,α_2), for a given squeeze parameter r, can have remarkably different values than does the set (β_1,β_2) in representing the same state.

III. BEAM SPLITTING AND MULTIPHOTON INTERFERENCE

We now consider the result of mixing the two output beams of the coherently stimulated down-converter at a 50:50 beam splitter. Of course, to maintain coherences and correlations, the output beams must propagate on equidistant paths to the beam splitter. Equal path lengths can be calibrated experimentally using the Hong-Ou-Mandel effect [2].

For convenience we assume that our beam splitter is balanced (50:50) and thus performs a transformation that can be described as $\pi/2$ rotation about the "1" axis as

given by $\hat{U}_{\rm BS} = \exp(-i\pi \hat{J}_1/2)$, were we have followed Yurke *et al.* [15], who use the Schwinger realization of the angular momentum algebra in terms of a pair of boson operators to describe beam splitters and some other linear optical devices. Our state after beam splitting, in the angular momentum representation, is thus given by

$$|\text{out,BS}\rangle = \hat{U}_{\rm BS}|z;\alpha_1,\alpha_2\rangle = \sum_{j=0}^{\infty}\sum_{m=-j}^{j}\sum_{m'=-j}^{j} c(j+m,j-m) i^{m'-m} d^j_{m',m}\left(\frac{\pi}{2}\right)|j,m'\rangle. \tag{29}$$

The probability after beam splitting that there are N_1 photons in mode 1 and N_2 in mode 2 is given by

$$P(N_1,N_2) = |\langle J,M \mid \text{out,BS1}\rangle|^2 = \left|\sum_{m=-J}^{J} c(j+m,j-m) i^{M-m} d^J_{M,m}\left(\frac{\pi}{2}\right)\right|^2, \tag{30}$$

for $N_1 = J + M$ and $N_2 = J - M$, where the $d^j_{m',m}(\varphi)$ values are the usual Wigner rotation functions [16]

$$d^j_{m',m}(\varphi) = \langle j,m'|\exp(-i\varphi \hat{J}_2)|j,m\rangle. \tag{31}$$

We now consider the effects of mixing the output beams of the down-converter at a beam splitter in the manner as sketched in Fig. 4. Again, we first consider the limiting case where the input coherent state amplitudes vanish so that we are dealing only with the TMSVS of Eq. (4) as the output. The output of the beam splitting is

$$|\text{out BS1}\rangle = (1-|\xi|^2)^{1/2}\sum_{n=0}^{\infty}\left(\frac{i\xi}{2}\right)^n \sum_{k=0}^{n}\left[\binom{2k}{k}\binom{2n-2k}{n-k}\right]^{1/2}|2k\rangle_a|2n-2k\rangle_b, \tag{32}$$

where we have used a result from Campos *et al.* [15] for the action of beam splitting on input twin-Fock states $|n\rangle_a|n\rangle_b$ with a suitable modification for our choice of representation for the first beam splitter. The joint photon-number distribution for this output state is presented in Fig. 5, where we notice that only the even number of states are populated. Some time ago, Gagen and Milburn [17] claimed that this was a reflection of strong correlations due to multiphoton interference. However, it has since been shown [18] that the output state of Eq. (32) is, in fact, not an entangled state at all and that the beam-splitting transformation causes a factorization of the input TMSVS into a product of single-mode squeezed vacuum states, neither of which has an odd photon-number state populated [19].

Recall that the TMSVS is a superposition of twin-Fock states $|n\rangle_a|n\rangle_b$ and thus contains perfect photon-number correlations. But this means that there is a very large uncertainty in their relative phases. By overlapping such states on a beam splitter, the phase fluctuations are converted into photon-number fluctuations in the sense that there is now a large uncertainty for the beam location of the photons: the probability of finding them in one beam or the other is relatively high. For the twin-Fock state input $|n\rangle_a|n\rangle_b$, the nonzero elements of the output photon-number distribution are given by

$$P(2k,2n-2k) = \binom{2k}{k}\binom{2n-2k}{n-k}\left(\frac{1}{2}\right)^{2n}, \quad k = 0,1,2,\ldots,n, \tag{33}$$

a distribution known in probability theory as the fixed-multiplicative discrete arcsine law of order n [20]. This distribution has the characteristic "U shape" in going from $k = 0$ to $k = n$, where the minimum occurs for $k = n/2$ for n even or $k = (n \pm 1)/2$ for n odd. Twin-Fock states as a resource for sub-standard quantum limited optical interferometry have been discussed by Holland and Burnett [21] and Campos *et al.* [22], where the latter considered the use of photon-number parity measurements for the detection scheme. The beam-splitter output distribution for input TMSVS is a collection of "U shapes" from each of the relevant input states $|n\rangle_a|n\rangle_b$, and an example is given in Fig. 6(a). It is evident that beam splitting results in a large uncertainty in the location of the photons with respect to the two output beams. The application of the TMSVS to interferometry has been studied by Anisimov *et al.* [4], who showed that sub-Heisenberg limited sensitivity for phase-shift measurements is possible. Later, Gerry and Mimih [23] studied the application to interferometry of yet another state that consists of a superposition of the correlated number state pairs $|n\rangle_a|n\rangle_b$, this being the pair coherent state [24]. In contrast to the TMSVS, the pair coherent states exhibit sub-Poissonian photon statistics in each mode. Recently, Spasibko *et al.* [25] experimentally examined the interference effects and photon-number fluctuations from TMSVS whose twin beams fall on opposite sides of a beam splitter.

Because the beam-splitter transformation results in a sum involving the amplitudes $c(j+m,j-m)$ as given in Eq. (29), the joint photon-number probability distribution given by Eq. (30) will generally depend not only on the angle Φ but also the individual angles θ_1,θ_2, and 2ϕ. We demonstrate this in Figs. 6(a) and 6(b) using the same squeezing and coherent state parameters as before and for the choice $\Phi = \pi/2$ with (a) $\theta_1 = \pi/2$, $\theta_2 = 0$, and $\phi = 0$ and with (b) $\theta_1 = 0$, $\theta_2 = \pi/2$, and $\phi = 0$. In both cases we notice asymmetric distributions with a tendency for the clustering on the photon-number states to be populated along the line $n_1 = 0$ for (a) and $n_2 = 0$

for (b). In Fig. 6(c) we display the case for the choices $\Phi = \pi, \theta_1 = \theta_2 = \pi/2$, and $\phi = 0$, which results in a distribution where population is symmetrically clustered along the lines $n_1 = 0$ and $n_2 = 0$. Distributions with this structure are known to be particularly conducive to achieving interferometric phase-shift measurements with sensitivities greater than the standard quantum limit $\Delta\varphi_{\rm SQL} = 1/\sqrt{N}$. From the heuristic number phase uncertainty relation, $\Delta N \Delta\varphi \simeq 1$ for a single mode of the field, and if the uncertainty in the photon number is on the order of the number of photons, $\Delta N \approx N$, which is the case in Fig. 6(c), then the uncertainty in the phase is given by $\Delta\varphi \sim 1/N$, the Heisenberg limit of sensitivity being $\Delta\varphi_{\rm HL} = 1/N$. The essential point is that in a distribution such as in Fig. 6(c) there is great uncertainty with regard to the location of most of the photons, an uncertainty created by the beam splitter and certain choices of phases θ_1, θ_2, and ϕ.

IV. APPLICATION TO INTERFEROMETRY

Here we assume the output beams of the down-converter are directed through a Mach-Zehnder interferometer, as indicated in Fig. 5. The relative phase shift between the two arms of the interferometer we denote as φ. We assume that photon-number parity measurements are performed on the output b mode. We follow Yurke *et al.* [15], taking the input state to the interferometer $|\text{in}\rangle$, which is related to its output state $|\text{out}\rangle$ according to

$$|\text{out}\rangle = e^{i\frac{\pi}{2}\hat{J}_1} e^{-i\varphi\hat{J}_3} e^{-i\frac{\pi}{2}\hat{J}_1} |\text{in}\rangle = e^{-i\varphi\hat{J}_2}|\text{in}\rangle, \tag{34}$$

where we have used the relation $e^{i\frac{\pi}{2}\hat{J}_1}\hat{J}_3 e^{-i\frac{\pi}{2}\hat{J}_1} = \hat{J}_2$. The parity operator of the output b mode is

$$\hat{\Pi}_b = (-1)^{\hat{b}^\dagger\hat{b}} = e^{i\pi\hat{b}^\dagger\hat{b}} = e^{i\pi(\hat{J}_0 - \hat{J}_3)}, \tag{35}$$

and its expectation value is given by

$$\langle\hat{\Pi}_b(\varphi)\rangle = \langle\text{out}|\hat{\Pi}_b|\text{out}\rangle = \langle\text{in}|e^{i\varphi\hat{J}_2}e^{i\pi(\hat{J}_0-\hat{J}_3)}e^{-i\varphi\hat{J}_2}|\text{in}\rangle. \tag{36}$$

For our input states this becomes

$$\begin{aligned}
&\langle\hat{\Pi}_b(\varphi)\rangle \\
&= \sum_{J=0}^{\infty}\sum_{M=-J}^{J} \langle\text{in}|e^{i\varphi\hat{J}_2}e^{i\pi(\hat{J}_0-\hat{J}_3)}|J,M\rangle\langle J,M|e^{-i\varphi\hat{J}_2}|\text{in}\rangle \\
&= \sum_{J=0}^{\infty}\sum_{M=-J}^{J} e^{i\pi(J-M)}\langle\text{in}|e^{i\varphi\hat{J}_2}|J,M\rangle\langle J,M|e^{-i\varphi\hat{J}_2}|\text{in}\rangle \\
&= \sum_{J=0}^{\infty}\sum_{M=-J}^{J} e^{i\pi(J-M)}\left|f_M^{(J)}(\varphi)\right|^2,
\end{aligned} \tag{37}$$

where

$$\begin{aligned}
f_M^{(J)}(\varphi) &= \langle J,M|e^{-i\varphi\hat{J}_2}|\text{in}\rangle \\
&= \sum_{j=0}^{\infty}\sum_{m=-j}^{j} c(j+m,j-m)\langle J,M|e^{-i\varphi\hat{J}_2}|j,m\rangle \\
&= \sum_{j=0}^{\infty}\sum_{m=-j}^{j} c(j+m,j-m)\langle J,M|e^{-i\varphi\hat{J}_2}|J,m\rangle\delta_{J,j} \\
&= \sum_{m=-J}^{J} c(J+m,J-m)d^J_{M,m}(\varphi).
\end{aligned} \tag{38}$$

The parity operator for the output a mode is

$$\hat{\Pi}_a = (-1)^{\hat{a}^\dagger\hat{a}} = e^{i\pi\hat{a}^\dagger\hat{a}} = e^{i\pi(\hat{J}_0+\hat{J}_3)} \tag{39}$$

and its output expectation value is

$$\langle\hat{\Pi}_a(\varphi)\rangle = \sum_{J=0}^{\infty}\sum_{M=-J}^{J} e^{i\pi(J+M)}\left|f_M^{(J)}(\varphi)\right|^2. \tag{40}$$

In Fig. 7 we plot $\langle\hat{\Pi}_b(\varphi)\rangle$ versus φ for the case where $r = 1.2$ and $\alpha_1 = \alpha_2 = 1$. It turns out that without phase-shift adjustments, the expectation values of the parity operators are not "centered" about $\varphi = 0$. To bring about such a centering, we require the phase transformations $\varphi \to \varphi + \pi/2$ for the case where $\Phi = 0$ and $\varphi \to \varphi - \pi/2$ for the case where $\Phi = \pi$, as can be accomplished with simple linear optical elements.

One could determine the uncertainty in the phase-shift measurement (the sensitivity) by the error propagation calculus according to

$$\Delta\varphi = \frac{(\Delta\Pi_b)}{|\partial\langle\hat{\Pi}_b(\varphi)\rangle/\partial\varphi|}, \tag{41}$$

where $\Delta\Pi_b = \sqrt{\langle\hat{\Pi}_b^2(\varphi)\rangle - \langle\hat{\Pi}_b(\varphi)\rangle^2}$ and where $\langle\hat{\Pi}_b^2(\varphi)\rangle = 1$. On the other hand, a computationally more efficient approach, especially for our states, is to calculate the minimum achievable uncertainty in the measurement of phase shifts as given by the quantum Cramer-Rao bound [13]

$$\Delta\varphi_{\rm min} = \frac{1}{\sqrt{F_Q}}, \tag{42}$$

where F_Q is the quantum Fisher information and is given as [14]

$$F_Q = 4[\langle\psi'(\varphi)\,|\,\psi'(\varphi)\rangle - |\langle\psi'(\varphi)\,|\,\psi(\varphi)\rangle|^2]. \tag{43}$$

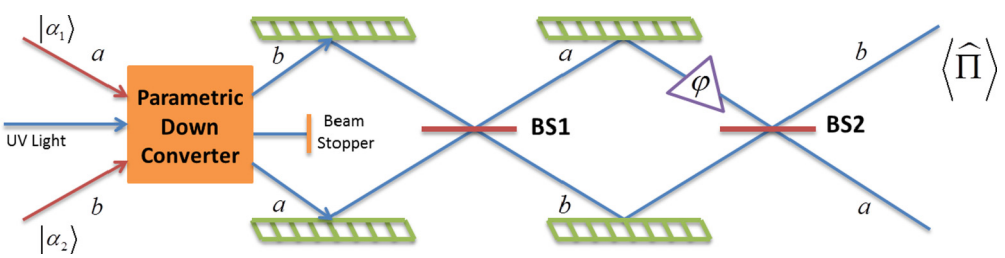

FIG. 5. (Color online) A sketch of our scheme for interferometric detection of the phase shift denoted φ via a Mach-Zehnder interferometer, the second on the right between the first and second beam splitters (BS1 and BS2, respectively), with two-mode squeezed coherent states as fed into BS1. Photon-number parity measurements are to be performed on the output b beam.

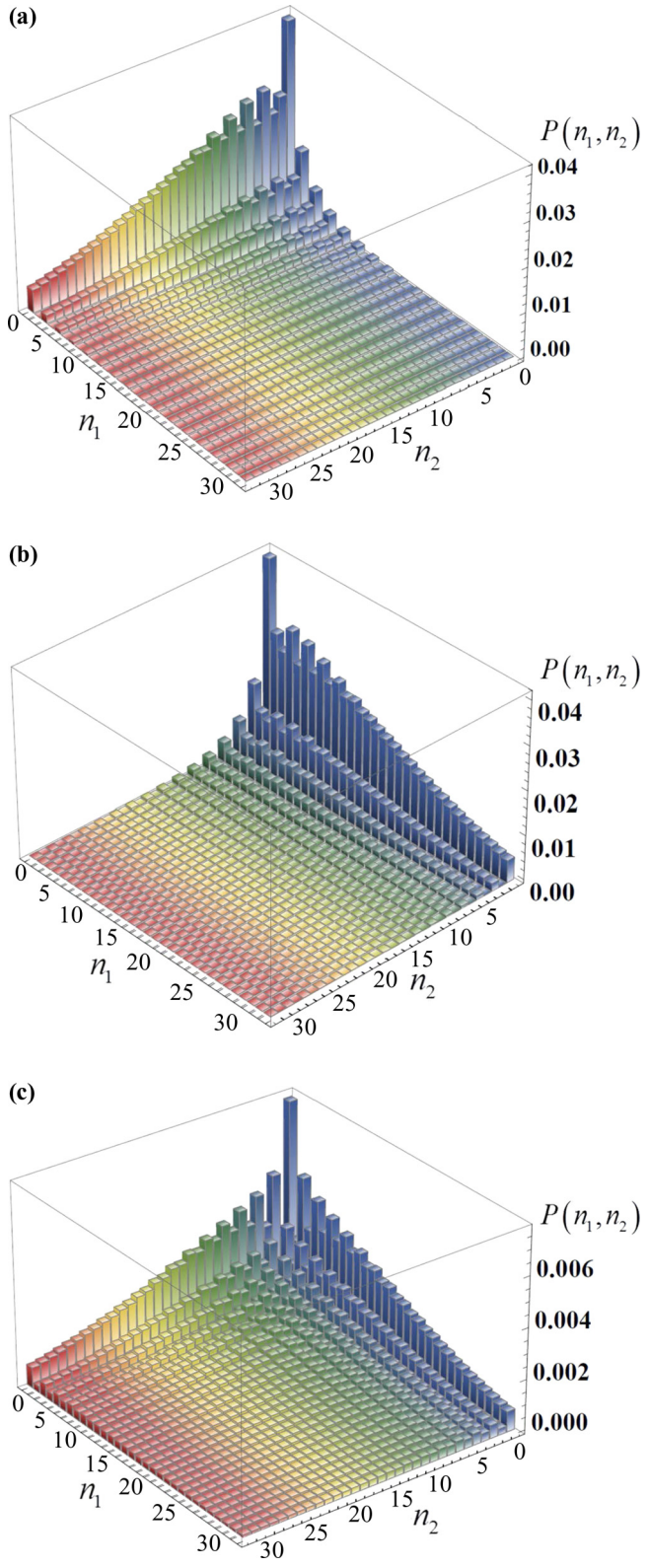

FIG. 6. (Color online) Joint photon-number distribution $P(n_1, n_2)$ versus n_1 and n_2 for $|\alpha_1| = |\alpha_2| = 1$, $r = 1.2$, and (a) $\Phi = \pi/2$ with $\theta_1 = \pi/2, \theta_2 = 0, \phi = 0$; (b) $\Phi = \pi/2$ with $\theta_1 = 0, \theta_2 = \pi/2, \phi = 0$; and (c) for $\Phi = \pi$, $\theta_1 = \pi/2, \theta_2 = \pi/2, \phi = 0$.

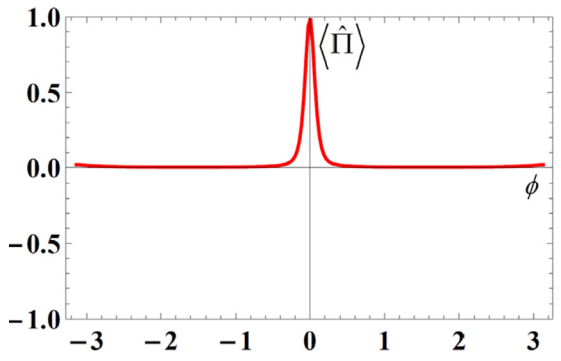

FIG. 7. (Color online) For the choices $r = 1.2$ and $\alpha_1 = \alpha_2 = 1$, the expectation value of the parity operator $\hat{\Pi}_b$ as a function of the phase shift φ for $\Phi = \pi$. To "center" the parity at $\varphi = 0$, we have in our calculations made the replacement $\varphi \to \varphi - \pi/2$. This shift can be made with appropriate linear optical elements.

Here $|\psi(\varphi)\rangle$ is the state vector just before the second beam splitter and

$$|\psi'(\varphi)\rangle = \frac{\partial}{\partial\varphi}|\psi(\varphi)\rangle. \tag{44}$$

For our case,

$$|\psi(\varphi)\rangle = e^{-i\varphi\hat{J}_3}e^{-i\frac{\pi}{2}\hat{J}_1}|\text{in}\rangle \tag{45}$$

and

$$|\psi'(\varphi)\rangle = -ie^{-i\varphi\hat{J}_3}\hat{J}_3e^{-i\frac{\pi}{2}\hat{J}_1}|\text{in}\rangle, \tag{46}$$

which leads to

$$\langle\psi'(\varphi)\,|\,\psi(\varphi)\rangle = i\langle\text{in}|\hat{J}_2|\text{in}\rangle \tag{47}$$

and to

$$\langle\psi'(\varphi)\,|\,\psi'(\varphi)\rangle = \langle\text{in}|\hat{J}_2^2|\text{in}\rangle, \tag{48}$$

where we have used the relation

$$e^{i\frac{\pi}{2}\hat{J}_1}\hat{J}_3e^{-i\frac{\pi}{2}\hat{J}_1} = \hat{J}_2. \tag{49}$$

Our expression for the quantum Fisher information becomes

$$F_Q = 4\langle(\Delta\hat{J}_2)^2\rangle_{\text{in}}, \tag{50}$$

where $\langle(\Delta\hat{J}_2)^2\rangle_{\text{in}}$ is the variance of the operator $\hat{J}_2$ with respect to the input state. In all cases studied so far, the quantum Cramer-Rao bound agrees with the phase uncertainty obtained from the error propagation calculus under the assumption that the photon-number parity operator is the relevant observable. We have compared our quantum Cramer-Rao bound results with sample error propagation calculus results based on the measurement of photon-number parity and have found complete agreement.

In Fig. 8 we plot an example of $\Delta\varphi_{\text{min}}$ versus $\bar{n}$ for the case where $\Phi = \pi$ and $r = 2$ and where $|\alpha|$ is being increased. The upper and lower dashed lines on each of the graphs represent the corresponding standard quantum limits (SQL), $\Delta\varphi_{\text{SQL}} = 1/\sqrt{\bar{n}}$, and Heisenberg limits (HL), $\Delta\varphi_{\text{HL}} = 1/\bar{n}$, respectively. We find that the noise reduction falls almost exactly along the curve for the Heisenberg limit.

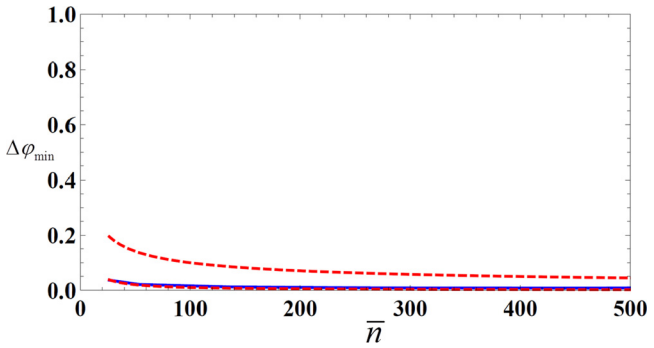

FIG. 8. (Color online) The phase uncertainty $\Delta\varphi_{\min}$ obtained via the Cramer-Rao bound versus the total average photon number for $\Phi = \pi$ and for $r = 2.0$. The upper and lower dashed lines represent, respectively, the corresponding standard quantum limits and Heisenberg limits of the phase-shift uncertainties.

V. CONCLUSIONS

In this paper, we have re-examined the two-mode squeezed coherent states (TMSCS) as obtained by the action of the two-mode squeeze operator representing the time evolution operator of the parametric down-conversion process acting on input coherent light fields. We have examined the role of the various phases that enter the state, that is, the phase of the classical pump field and the two phases associated with the input coherent states of the parametric down-conversion process, and as to how these phases appear depending on the definition of the state, whether as two-mode squeezed coherent states as in Eq. (10) or as displaced TMSVS as given in Eq. (16). We have investigated the effect the phases have on the joint photon-number probability distributions of the TMSCS and on other statistical properties such as the average photon number. Furthermore, we have studied the results of mixing the two beams of the TMSCS with a 50:50 beam splitter and have examined the means of controlling that output by making certain choices of the various phases. And finally, we have examined the prospect of utilizing the TMSCS for photon-number parity–based interferometry, and have found, for certain choices of parameters and phases, noise reductions approaching the level of the Heisenberg limit.

In this work we have considered the pump field of the down-converter to be a classical prescribed field, which means we have ignored the effects of photon depletion the pump field altogether. In future work we shall study the states produced in the case where the pump field is quantized and assumed to be initially in a coherent state or some form of single-mode pure nonclassical state such as a squeezed vacuum. It will be interesting to explore the effects of the phases on the evolution of the fully quantized model, especially their effects on the photon-number distributions and on the average photon numbers of the output in the signal and idler modes. For the case where all fields are initially in coherent states and with phase choices such that $\Phi = \pi$, we would expect a more rapid decrease in the average photon number of the pump field as the average photon numbers of the signal and idler modes increase compared to the case when $\Phi = 0$. In fact, we expect that the parametric approximation breaks down after a short time such that the very high average photon numbers appearing in the output signal and idler modes cannot be realized in practice. On the other hand, projective state reductions performed on the output pump beam at different times should open up the prospects for new forms of nonclassical, entangled, two-mode field states.

ACKNOWLEDGMENT

This work was partially supported by a grant from PSC-CUNY.

APPENDIX: PHASE RELATIONS AND THE U(1) ⊗ U(1) INVARIANCE OF PHOTON-NUMBER PROBABILITY DISTRIBUTIONS

We first establish a connection between the phases $\Phi = \theta_1 + \theta_2 - 2\phi$ and $\Psi = \psi_1 + \psi_2 - 2\phi$. We begin by considering the quantity $\alpha_1\alpha_2 e^{-2i\phi}$ occurring three places in the coefficients given in Eq. (25) by substituting for α_1 and α_2 from Eq. (20) to yield the relation

$$\alpha_1\alpha_2 e^{-2i\phi} = |\alpha_1||\alpha_2|e^{i\Phi} = \tfrac{1}{2}(|\beta_1|^2 + |\beta_2|^2)\sinh(2r) + |\beta_1||\beta_2|[\cos\Psi\cosh(2r) + i\sin\Psi]. \tag{A1}$$

By equating the real and imaginary parts of Eq. (A1) we find that

$$\Phi = \tan^{-1}\left[\frac{2|\beta_1||\beta_2|\sin\Psi}{2|\beta_1||\beta_2|\cosh(2r)\cos\Psi + (|\beta_1|^2+|\beta_2|^2)\sinh(2r)}\right]. \tag{A2}$$

Conversely, by considering the combination $\beta_1\beta_2 e^{-2i\phi}$ and substituting from Eq. (19) we have

$$\beta_1\beta_2 e^{-2i\phi} = |\beta_1||\beta_2|e^{i\Psi} = -\tfrac{1}{2}(|\alpha_1|^2 + |\alpha_2|^2)\sinh(2r) + |\alpha_1||\alpha_2|[\cos\Phi\cosh(2r) + i\sin\Phi], \tag{A3}$$

from which it follows that

$$\Psi = \tan^{-1}\left[\frac{2|\alpha_1||\alpha_2|\sin\Phi}{2|\alpha_1||\alpha_2|\cosh(2r)\cos\Phi - (|\alpha_1|^2+|\alpha_2|^2)\sinh(2r)}\right]. \tag{A4}$$

Note that the phases Φ and Ψ as related through Eqs. (A2) and (A4) are, in general, nonlinear functions of each other. Selvadoray *et al.* [10] have identified Φ as the Gouy phase [26] for the TMSCS.

Finally, it has been noted that there exists a U(1) invariance of the photon-number distributions of single-mode squeezed coherent field states [27] and of the U(1) $\otimes$ U(1) invariance of the joint photon-number distributions of two-mode squeezed coherent states [10]. The invariance in the latter case is such that the photon-number probabilities depend only on the three phases through the combination $\Phi = \theta_1 + \theta_2 - 2\phi$ for the state definition given by Eq. (10) or the combination $\Psi = \psi_1 + \psi_2 - 2\phi$ through the definition of Eq. (16). However, this is rather trivial. For any pure two-mode field state given as

$$|\eta\rangle = \sum_{n=0}^{\infty}\sum_{m=0}^{\infty} B_{nm}|n\rangle_a|m\rangle_b, \tag{A5}$$

with joint photon-number distribution $P_{nm} = |B_{nm}|^2$, the U(1)$\otimes$ U(1) transformation is given by the operation [10]

$$\exp(i\zeta_1\hat{a}^\dagger\hat{a})\exp(i\zeta_2\hat{b}^\dagger\hat{b})|\eta\rangle = \sum_{n=0}^{\infty}\sum_{m=0}^{\infty}\exp[i(\zeta_1 n + \zeta_2 m)]B_{nm}|n\rangle_a|m\rangle_b, \tag{A6}$$

from which it is obvious that the transformed state has the same photon-number distribution as that of Eq. (A5). Thus, if the probabilities $P_{nm} = |B_{nm}|^2$ depend only on phases through the combinations Φ or Ψ, that will be trivially true for the transformed state of Eq. (A6). But, again, only incoherent properties of the state, the photon-number distribution or the average photon number, are invariant under the transformations. Quantities involving the coherences will strongly depend on the individual phases.

[1] For recent reviews, see, for example, M. Hillery, Acta Physica Slovaca **59**, 1 (2009); P. D. Drummond and M. Hillery, *The Quantum Theory of Nonlinear Optics* (Cambridge University Press, Cambridge, UK, 2014), and references therein.

[2] C. K. Hong, Z. Y. Ou, and L. Mandel, Phys. Rev. Lett. **59**, 2044 (1987).

[3] See, for example, Z. Y. Ou and L. Mandel, Phys. Rev. Lett. **61**, 50 (1988); Y. H. Shih and C. O. Alley, *ibid.* **61**, 2921 (1988); A. Kuzmich, I. A. Walmsley, and L. Mandel, *ibid.* **85**, 1349 (2000).

[4] P. M. Anisimov, G. M. Raterman, A. Chiruvelli, W. N. Plick, S. D. Huver, H. Lee, and J. P. Dowling, Phys. Rev. Lett. **104**, 103602 (2010).

[5] F. De Martini and F. Sciarrino, Prog. Quantum Electron. **29**, 165 (2005); S. L. Braunstein and P. van Loock, Rev. Mod. Phys. **77**, 513 (2005).

[6] See, for example, L. A. Lugiato, A. Gatti, and E. Brambilla, J. Opt. B: Quantum Semiclass. Opt. **4**, S176 (2002).

[7] See, for example, C. C. Gerry and P. L. Knight, *Introductory Quantum Optics* (Cambridge University Press, Cambridge, UK, 2005), p. 182.

[8] S. M. Barnett and P. K. Knight, J. Opt. Soc. Am. B **2**, 467 (1985); B. Yurke and M. Potasek, Phys. Rev. A **36**, 3464 (1987).

[9] C. M. Caves, C. Zhu, G. J. Milburn, and W. Schleich, Phys. Rev. A **43**, 3854 (1991).

[10] M. Selvadoray, M. S. Kumar, and R. Simon, Phys. Rev. A **49**, 4957 (1994). Their Eq. (17) contains a typo which we have corrected here. The phase factor $\exp[-i\pi(j - |m|)/2]$ has been replaced by $\exp[-i\pi(j - |m|)]$, which brings it into agreement with their Eq. (18).

[11] A. N. Boto, P. Kok, D. S. Abrams, S. L. Braunstein, C. P. Williams, and J. P. Dowling, Phys. Rev. Lett. **85**, 2733 (2000).

[12] A. Kolkiran and G. S. Agarwal, Opt. Express **16**, 6479 (2008); see also E. M. Nagasako, S. J. Bentley, R. W. Boyd, and G. S. Agarwal, Phys. Rev. A **64**, 043802 (2001); G. S. Agarwal, K. W. Chan, R. W. Boyd, H. Cable, and J. W. Dowling, J. Opt. Soc. Am. B **24**, 270 (2007).

[13] C. W. Helstrom, *Quantum Detection and Estimation Theory* (Academic Press, New York, 1976); S. L. Braunstein and C. M. Caves, Phys. Rev. Lett. **72**, 3439 (1994).

[14] See, for example, Y. Ben-Aryeh, J. Opt. Soc. B **29**, 2754 (2012).

[15] See M. E. Rose, *Elementary Theory of Angular Momentum* (Wiley, New York, 1957), p. 52.

[16] See B. Yurke, S. L. McCall, and J. R. Klauder, Phys. Rev. A **33**, 4033 (1986); R. A. Campos, B. E. A. Saleh, and M. C. Teich, *ibid.* **40**, 1371 (1989).

[17] M. G. Gagen and G. J. Milburn, Opt. Commun. **76**, 253 (1989).

[18] V. Bužek and M. Hillery, Czech. J. Phys. B **45**, 711 (1995); B. Böhmer and U. Leonhardt, Opt. Commun. **118**, 181 (1995); C. C. Gerry and A. Benmoussa, Phys. Rev. A **62**, 033812 (2000).

[19] See, for example, Ref. [7], p. 161.

[20] See, W. Feller, *An Introduction to Probability Theory and Its Applications* (Wiley, New York, 1957), Vol. 1, p. 77.

[21] M. J. Holland and K. Burnett, Phys. Rev. Lett. **71**, 1355 (1993).

[22] R. A. Campos, C. C. Gerry, and A. Benmoussa, Phys. Rev. A **68**, 023810 (2003).

[23] C. C. Gerry and J. Mimih, Phys. Rev. A **82**, 013831 (2010).

[24] G. S. Agarwal, Phys. Rev. Lett. **57**, 827 (1986); J. Opt. Soc. Am. B **5**, 1940 (1988).

[25] K. Yu. Spasibko, F. Töppel, T. Sh. Iskhakov, M. Stobińska, M. V. Chekhova, and G. Leuchs, New J. Phys. **16**, 013025 (2014).

[26] G. Gouy, C. R. Acad. Sci. **110**, 1251 (1890).

[27] B. Dutta, N. Mukunda, R. Simon, and A. Subramanian, J. Opt. Soc. B **10**, 253 (1993).